# Multi-aircraft Rerouting Method Under Dangerous Weather

Yukun Zheng , Ying Wang, Yun Sun, Yao Qi, and Ning Wang

*College of Equipment Management and Unmanned Aerial Vehicle Engineering, Air Force Engineering University, 32018 Xi'an, CHINA*

**Abstract.** In view of the problems that single-aircraft rerouting method existing in civil aviation considered little about the associated effects of multi-aircraft and route network characteristics. A multi-aircraft rerouting method under dangerous weather was proposed. Based on the characteristics of network failures during the occurrence of dangerous weather, the performance indicators and related constraints of temporary routes are analyzed to establish a single- aircraft rerouting model. Then, a multi-aircraft rerouting model based on layout of diversion points was proposed in combination with the performance indicators of the rerouted route network, and solved by NSGA-III algorithm. Finally, a simulation analysis was conducted using the regional flight route network in part of the Beijing Flight Information District as an example and the results show that multi-aircraft rerouting method can effectively avoid flight conflicts and improve the comprehensive characteristics of the network.

## 1 INTRODUCTION

The structure of China's airspace is complex. There are a large number of "no-fly zones", "restricted zones" and "danger zones" around the route. The sudden dangerous weather may block the route, which has a major impact on the flight safety of civil aviation[1]. In order to solve such problems, it is necessary to reroute the original route.

At present, domestic and foreign scholars have conducted preliminary studies on the problem of rerouting under dangerous weather. Yang Shuangshuang[2] adopted a geometric method to reroute under static dangerous weather. Wang Fei and Wang Lili[3-5] aim at minimizing the cost of rerouting, and established a rerouting model based on genetic algorithm, which improves the accuracy of rerouting planning. Meng Linghang[6] considered the dynamic characteristics of dangerous weather and designed a heuristic algorithm for the specific weather conditions. Li Xiong[7] proposed a multi-target rerouting model, but it was not universal. Luitpold Babe[8] and Wang Shijin[9] introduced the route terminal area into rerouting plan and established a three-dimensional model that circumvents the "three zones," but the model didn't consider the impact of sudden dangerous weather.

The current researches are mostly single-aircraft rerouting under dangerous weather without considering the relevance of rerouted routes and the integrity of route network which increase the possibility of flight conflicts. Based on single-aircraft rerouting, this paper proposes a multi-aircraft rerouting model based on the layout of diversion points, and uses a NSGA-III algorithm to solve the multi-object rerouting model.

## 2 SINGLE-AIRCRAFT REROUTING

### 2.1 Rerouting Environment Construction

In order to express the structural characteristics of the aeronautical domain, use the grid method to characterize the rerouting environment[9]. The target airspace is represented as a mesh structure composed of several grids, as shown in Figure1 , and its specific steps are:

(1) Create a grid coordinate network according to the connection between origin and destination of rerouting.

(2) Divide the grid coordinate network into $(G_x+2)\times G_y$ square grid. The side length of grid is $m'$, and the label is $n_i$.

(3) Assign a specific state value for each grid to indicate the security, and use center point state to represent the grid state.

$$C(n_i)=\begin{cases}1 & n_i \in Z_U \cup Z_W \\ 0 & n_i \in Z_{free}\end{cases} \tag{1}$$

In the formula, $C(n_i)$ is state assignment function, $Z_U$ represents the "three zones" airspace, $Z_W$ represents the dangerous weather scope, and $Z_{free}$ represents free airspace.

(4) Display dangerous weather scope and the "three zone" airspace in the grid network, and the schematic diagram is as follows:

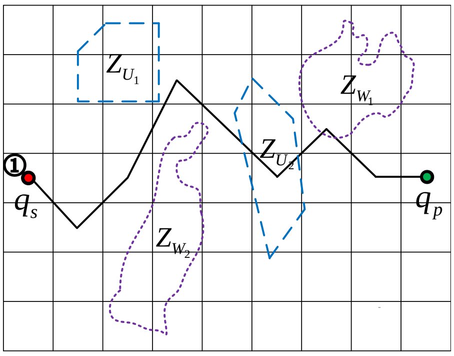


**Figure 1.** Rerouting environment diagram

In the figure, $q_s$ is original, $q_p$ is destination, and ① indicates the air route.

### 2.2 Objective Functions and Constraints

The traditional single-aircraft rerouting uses the shortest route distance as the planning objective, which only considers the economic effects while ignoring its safety. Therefore, this paper adopts three objective functions: shortest route distance, minimum route dispersion degree and minimum route slope change amount to enhance the safety, adaptability and stability of the rerouting method. Then introduce a penalty function to ensure the rerouted route meets the obstacle avoidance constraints and range constraints, which are expressed as follows:

$$\min D = d\left(q_s , q_1\right) + d\left(q_{G_x} , q_p\right) + \sum_{i=1}^{G_x-1} d\left(q_i , q_{i+1}\right) + \Phi \tag{2}$$

$$\min S = \left[\left(y_s - \bar{y}\right)^2 + \left(y_p - \bar{y}\right)^2 + \sum_{i}^{G_x}\left(y_i - \bar{y}\right)^2\right] \times \left[1/\left(G_x + 2\right)\right] + \Phi \tag{3}$$

$$\min K = \left|k_{q_1q_2} - k_{sq_1}\right| + \sum_{i=2}^{G_{x-1}}\left|k_{q_iq_{i+1}} - k_{q_{i-1}q_i}\right| + \left|k_{q_{G_x}p} - k_{q_{G_x-1}q_{G_x}}\right| + \Phi \tag{4}$$

$$\Phi = \lambda \cdot \left(C\left(d'_{sq_1}\right) + \sum_{i=1}^{G_x}\sum C\left(d'_{q_iq_{i+1}}\right) + C\left(d'_{q_{G_x}p}\right)\right) \tag{5}$$

Among them, $q_i$ represents a grid the rerouted route passed, $D$ represents the total distance, $d\left(q_i , q_{i+1}\right)$ represents the distance of $q_iq_{i+1}$ . S represents dispersion degree of the route, $y_i$ is the ordinate of the grid. $K$ represents slope change of the route, $k_{q_iq_{i+1}}$ is the slope of $q_iq_{i+1}$ . $\Phi$ represents the penalty function, and $\lambda$ is a penalty factor, preferably 1000[7], $d'_{q_iq_{i+1}}$ represents the passing grid collection, $\sum_{i=1}^{G_x} C\left(d'_{q_iq_{i+1}}\right)$ represents state values of rerouted route. At the same time, in order to ensure the rerouted route meets actual needs, the corresponding constraints are proposed:

$$\left(sq_1 \cup q_iq_j \cup q_{G_x}p\right) \notin \left(Z_T \cup Z_W\right) i, j \in \left[1, G_x\right] \tag{6}$$

$$q_i \in Z \quad i \in \left[1, G_x\right] \tag{7}$$

$$m' \geq 10\text{km}^{[8]} \tag{8}$$

Equations (6), (7), and (8) represent obstacle avoidance constraints, optimization range constraints, and grid length constraints, respectively.

### 2.3 Algorithm coding

Because the binary code will limit the rerouting angle, when using a multi-objective algorithm to solve the model, the objective function can be compiled by using integer coding. Set the chromosome length to $G_x$ , so the gene value range is $\left[1, G_y\right]$. The route of chromosome 434654544 is shown as ① in figure 1.

## 3 MULTI-AIRCRAFT REROUTING

### 3.1 Model Assumptions

The rerouted route is also referred as temporary route. When a large-scale dangerous weather occurs in a regional route network and affects the operation of aircraft, a temporary route network for multi-aircraft rerouting may be formed on the basis of single-aircraft rerouting, and a optimization model based on diversion point layout to optimizes the network to reduce flight conflicts and improve the security can be adopted. To simulate the actual operating environment, make the following assumptions:

(1) Aircraft in the network are all located at the same height level.

(2) The connection relationship and flight flow between the waypoints remain unchanged, and the “three zones” and dangerous weather areas cannot be crossed.

(3) The aircraft cruise speed is 800km/h, the specified minimum radar control interval is 20km, and the optimal range of waypoints is $\pm 80$ km.

(4) The cost of network optimization is not considered.

### 3.2 Structure of Temporary Route Network

The regional temporary route network consists of waypoints and route segments. The waypoints include airport, intersections points, and diversion points. Route segments are connected by waypoints. In order to reflect the properties of the temporary route network, it can be expressed as $N\left(P, D', f\right)$, and its meaning is as follows:

(1) $P = \left\{P_1, \cdots, P_n, \cdots P_{n+m}, \cdots P_{n+m+k}\right\}$ represents the set of waypoints, the former $n$ is airport, the middle $m$ is intersection points, and the latter $k$ is diversion point.

(2) $D'$ is total distance of the temporary routes which can be expressed as:

$$D_l' = \sum d_{ij} \tag{9}$$

In the formula, $d_{ij}$ means the distance of segment $P_iP_j$, $\sum d_{ij}$ is the sum of segment distance values that make up the network.

(3) $f$ is the network flow parameters, including $f_{ij}$ represents the segment flow of $P_iP_j$ and $f_i$ represents the waypoint flow of $P_i$.

### 3.3 Objective Functions and Constraints

In order to improve economy of the temporary route network while ensuring its security, the minimum operating cost, minimum flight collision coefficient, and minimum route angle change are used as the objective functions of the network optimization and can be expressed as follows:

$$\min T = \sum_{l=1}^{h} f_l D_l' + \Phi' \tag{10}$$

$$\min c = \sum_{i=n+1}^{m+n} \sum_{j=1}^{m+n+k} \sum_{k=j+1}^{m+n+k} \left[ \left( 2 f_{ji} f_{ki} / v \right) \cdot L_{\min} \cdot \arccos\left( \alpha_{jik}/2 \right) / \left( f_{ji} + f_{ki} \right) \right] + \Phi' \tag{11}$$

$$\min \theta = \sum \Delta\theta_l + \Phi' \tag{12}$$

In these formulas, $T$ is operating cost, $f_l$ is flow of the temporary route $l$ , $h$ is the number of temporary routes, $c$ is the network flight collision coefficient which is ralated to the angle and flow rate of air route segment, $v$ is aircraft cruise speed, $L_{\min}$ is minimum control distance, $\alpha_{jik}$ is the angle between segment $P_jP_i$ and $P_kP_i$. $\theta$ is angle change of temporary routes in the network, and $\Delta\theta_l$ is the angle change of $l$. $\Phi'$ is a penalty function, expressed as follows:

$$\Phi' = \lambda \cdot \sum C(l) \tag{13}$$

In the formula, $\sum C(l)$ represents the sum of the status values of all the temporary routes.

Combined with the actual needs of network optimization, the following constraints are proposed:

$$l \cap \left( Z_W \cup Z_U \right) = \varnothing \tag{14}$$

$$x_i^{\min} \le x_i \le x_i^{\max} \text{ , } y_i^{\min} \le y_i \le y_i^{\max} \tag{15}$$

Among them, Equations (14) and (15) represent obstacle avoidance constraints and optimization scope constraints respectively. $(x_i, y_i)$ is the coordinate of $P_i$ , $x_i^{\min}$, $x_i^{\max}$ are the abscissa optimization range of $P_i$, and $y_i^{\min}$, $y_i^{\max}$ are the ordinate optimization range of $P_i$.

### 3.4 Algorithm coding

The structure of the temporary route network mainly depends on the layout of the diversion points, and a real-coded method can be used to construct chromosomes to represent their location information, for example: $x_{11}x_{12}\cdots x_{\alpha 1}x_{\alpha 2}\cdots x_{k1}x_{k2}$ . Where $k$ is the number of diversion points, $2k$ is the length of the chromosome, and $x_{\alpha 1}$ , $x_{\alpha 2}$ are the horizontal and vertical coordinates of point $P_\alpha$.

## 4 REROUTING ALGORITHM DESIGN BASED ON NSGA-III

### 4.1 Basic ideas

Common multi-objective optimization algorithms include multi-objective weighted genetic algorithm, target vector method, etc. Mostly, the multi-objective problem is transformed into a single-objective problem through transformational ideas. The NSGA-III algorithm can obtain the pareto optimal solution of the NP complete problem[10]. This non-inferior optimal solution set is suitable for different decision-making environments and enhances the completeness, robustness and comprehensiveness of the decision-making scheme. On the basis of inheriting the NSGA-II non-dominated sorting operation, the method of solving the reference distance by the association operation replaces the original congestion operator, avoids the premature convergence of the algorithm and improves the population diversity, when the number of objective functions is greater than 3, the planning effect is obviously better than the traditional multi-objective planning algorithm.

### 4.2 Operators

Combined with the actual needs of network optimization, the following operator can be set:

(1) Selecting operator: Use the roulette selection method and the objective function is set as a fitness function. The higher the fitness, the greater the probability of individual selection.

(2) Crossover operator: Use a method of partial match crossover, the cross points and matching segments of two parent individuals are determined to achieve chromosome rearrangement.

(3) Mutation operator: Adopt the basic mutation operation to randomly select a gene on the chromosome and change its value.

(4) Removing operator: Perform a delete operation on the chromosome whose coordinates of the waypoint is out of range, and regenerate the chromosome.

### 4.3 Algorithm Steps

The basic steps of the NSGA-III algorithm are similar to the traditional genetic algorithm[10], but there are innovations in selecting mechanism, as shown in Figure 2.

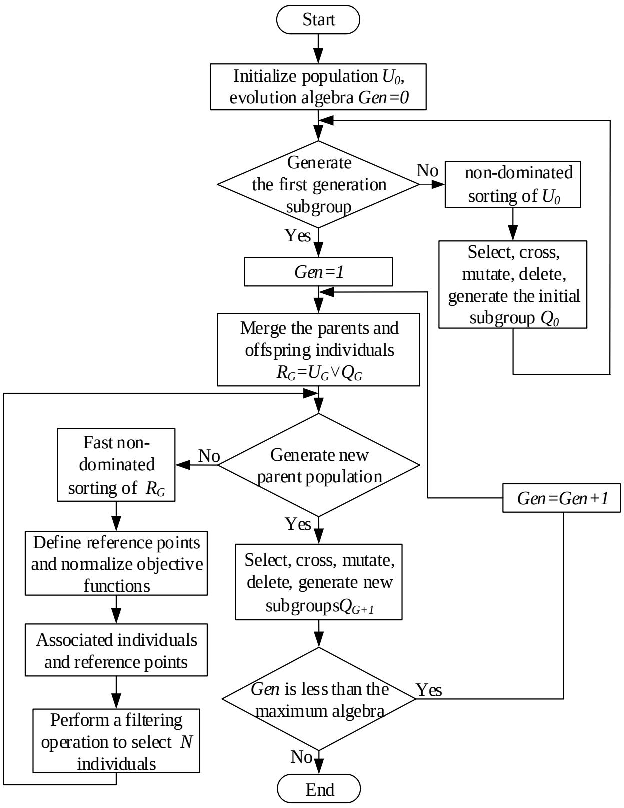


**Figure 2.** NSGA-III algorithm flow chart

## 5 SIMULATION ANALYSIS

Beijing flight information region is complex and the "three districts" are densely distributed. When dangerous weather occurs, it is easy to cause obstructions. Therefore, the routes of G212, B251, W41, H8, and B458 in this region are used as examples for simulation analysis. Its route information is shown in Table 1.

**Table 1.** Route information

| origin-destination | air route | flow sor/h |
|---|---|---|
| Taiyuan-Gubeikou | G212 | 8.4 |
| Taiyuan-Dawangzhuang | B251 | 9.9 |
| Dawangzhuang-Gubeikou | W41 | 7.7 |
| Pingyi - Shijiazhuang | H8 | 9.2 |
| Tianzhen - Shijiazhuang | B458 | 8.1 |

Among them, the straight distance from Taiyuan-Gubeikou on the G212 route is 506.61km. For convenience, the entire rerouting area is set to $22 \times 10$ grid coordinate network and $m' = 24.14$ km. Assume that the aircraft move from left to right or from top to bottom, when scattered thunderstorms occur in the area, carry out single-aircraft rerouting of 5 routes and collect them together, the network shown in Figure 3 is available.

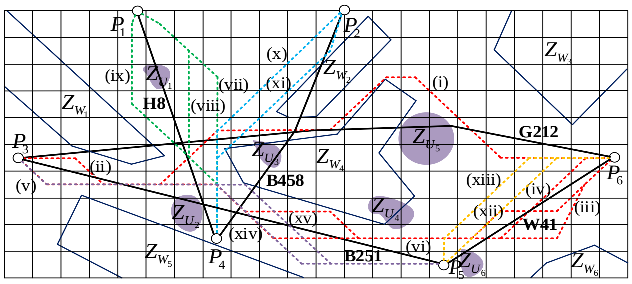


**Figure 3.** Schematic summary of single-route diversion routes

In the figure, the black solid line is the original route, and the red, purple, yellow, green, and blue dotted lines represent the reroute routes of G212, B251, W41, H8, and B458, respectively. Take optimal individual components of each rerouted route to form initial network of multi-aircraft rerouting, as shown in Figure 4.

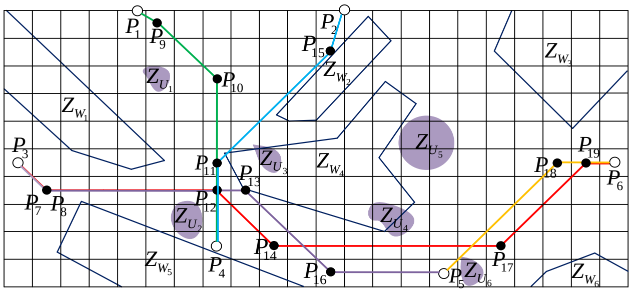

**Figure 4.** Initial network of multi-aircraft rerouting

In the figure, $P_i\left(i=1,\cdots 6\right)$ is airport point or border point, and $P_i\left(i=7,\cdots 19\right)$ is diversion point. It is easy to see the initial network composed of single-aircraft rerouting based on grid integer coding is complex and complicated, many routes overlap, and the distance is large. Therefore, it is necessary to carry out multi-aircraft rerouting of the initial network based on the existing diversion points. Set the number of populations to 100, the evolutionary generation to 800, the mutation rate to 0.1, and the hybridization rate to 0.15. Use NSGA-II, NSGA-II and particle swarm optimization algorithm to solve the multi-aircraft rerouting model, the network is shown in Figure 5.

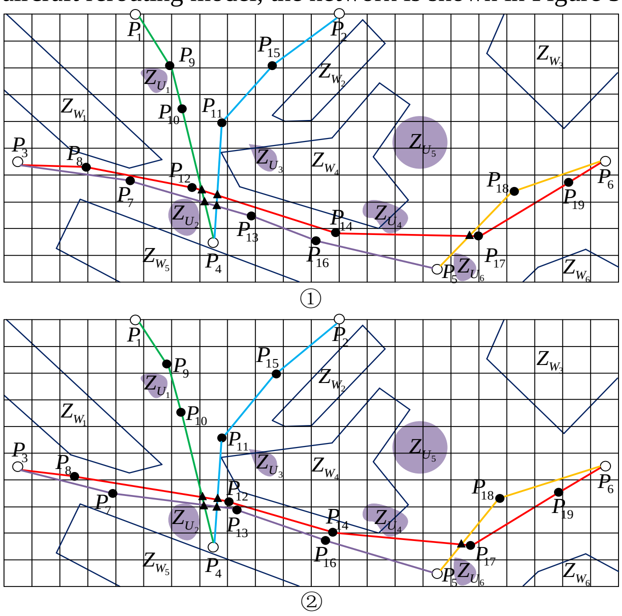

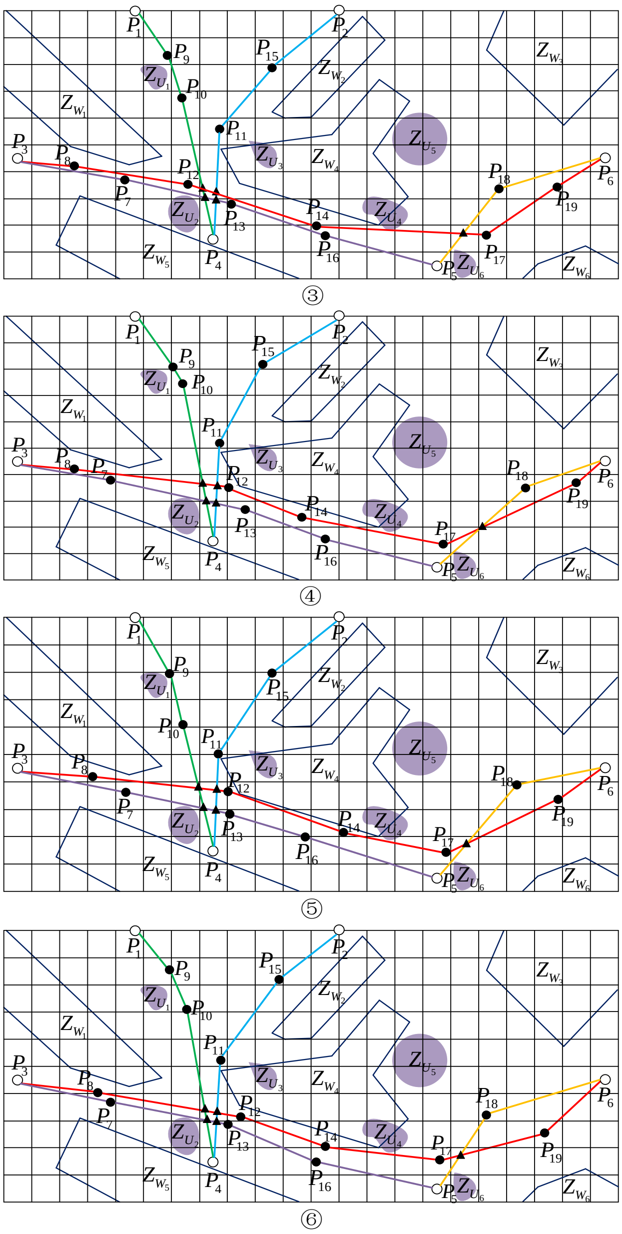


**Figure 5.** Multi-aircraft rerouting optimization network

Among them, ①-③ are the networks obtained by NSGA-III algorithm, ④ and ⑤ are the networks obtained by NSGA-II algorithm, and ⑥ is the network obtained by particle swarm algorithm. After judgment, all networks meet obstacle avoidance constraints and optimization scope constraints. The specific characteristic values are shown in Table 2.

**Table 2.** Characteristic value of networks

| No. | operating cost | flight conflict coefficient | angle change/ degree |
|---|---|---|---|
| ① | 13596 | 1.01 | 180.1 |
| ② | 13601 | 0.95 | 179.1 |
| ③ | 13640 | 1.03 | 178.0 |
| ④ | 13636 | 1.04 | 198.5 |
| ⑤ | 13626 | 1.06 | 191.0 |
| ⑥ | 13656 | 0.98 | 212.5 |
| ⑦ | 14326 | 1.58 | 533.7 |

In the table, ⑦ represents the initial network. By comparison, all the optimized networks are better than the initial network. Among them, the indicators of the networks ①、② and ③ are relatively balanced, and their optimization effect is the best. Some indicators of networks ④ and ⑤ are good, but they are slightly worse in overall integrity. The flight conflict coefficient of network ⑥ is smaller, but its other indicators rank lower. To further highlight the differences, the indicators of each optimized network are divided by the indicators of network ⑦ and make a contrast, as shown in Figure 5.

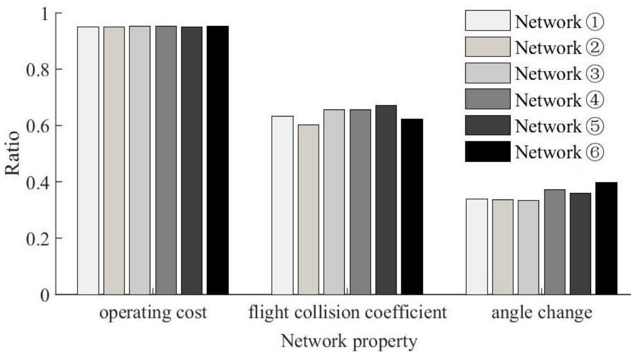


**Figure 5.** performance comparison

It is easy to see that network ② has the best improvement effect. Its operating cost is reduced by 5%, the flight conflict coefficient is reduced by 39.9%, and the angle change amount is reduced by 66.4%. Therefore, the NSGA-III algorithm can effectively solve the problem of multi-aircraft rerouting based on layout of diversion points and improve the safety and integrity of the temporary route network. What's more, a single operation can provide a variety of attributes with different results which can promote planning personnel to change the route design under different constraints and mission objectives.

## 6 Conclusion

This paper establishes a multi-aircraft rerouting model to study the route network under dangerous weather, which solves the problems of single-aircraft rerouting effectively and improves the safety and integrity of the temporary route network. Finally, the simulation analysis proves the validity of NSGA-III algorithm in solving multi-objective optimization problem, It can help to reduce the operating cost, flight conflict coefficient and angle change amount effectively which provides a new way for airspace rerouting planning.

## References

1. W Yan, Y Wang, Y F Meng. Journal of air force engineering university, 18, 6: 20-16 (2017)
2. S S Yang, Y Tian, L L Wan. Mathmetical in practice and theory, **42,** 13: 87-93 (2012)
3. F Wang, H Y Wang. TSEIT, **14**, 5: 154-160 (2014)
4. L L Wang, X Wang, B Peng. Flight Dynamics, **35**, 2: 84-87 (2017)

5. L L Wang, J Zhou. J. Wuhan. Univ. Technol, **36**, 5: 86-90 (2014)
6. L H Meng, X H Xu, S M Li, Z X Geng. J. Southwest.Jiaotong. Univ, **47**, 4: 686-691 (2012)
7. X Li, X H Xu, Y F Zhao, D X Wei. Act. Aer. ET. Astr. S, Acta. Aeronaut. Astronaut. Sin, **30**, 12: 2342-2347 (2009)
8. 8Babe Luitpold. J. Intell. Robot. Syst, **71**: 255-269 (2013)
9. S J Wang, Q Y Li, X Cao, H Y Li. Trans. N. Univ. Aeronaut. Astronaut, **33**, 4: 469-478 (2016)
10. D Kalyanmoy, J Himanshu. IEEE. T. Evolut. Comput, **18**, 4: 577-601. (2014)